



HAL
open science

Local to continental scale coupled fire-atmosphere simulation of large industrial fire plume

Roberta Baggio, Jean Baptiste Filippi, Benjamin Truchot, Flavio Couto

► To cite this version:

Roberta Baggio, Jean Baptiste Filippi, Benjamin Truchot, Flavio Couto. Local to continental scale coupled fire-atmosphere simulation of large industrial fire plume. *Fire Safety Journal*, 2022, 134, pp.103699. 10.1016/j.firesaf.2022.103699 . hal-03866875

HAL Id: hal-03866875

<https://hal.science/hal-03866875>

Submitted on 23 Nov 2022

HAL is a multi-disciplinary open access archive for the deposit and dissemination of scientific research documents, whether they are published or not. The documents may come from teaching and research institutions in France or abroad, or from public or private research centers.

L'archive ouverte pluridisciplinaire **HAL**, est destinée au dépôt et à la diffusion de documents scientifiques de niveau recherche, publiés ou non, émanant des établissements d'enseignement et de recherche français ou étrangers, des laboratoires publics ou privés.

Local to continental scale coupled fire-atmosphere simulation of large industrial fire plume

Roberta Baggio^a, Jean Baptiste Filippi^a, Benjamin Truchot^b and Flavio T. Couto^c

^a*SPE—Sciences Pour l'Environnement, Université de Corse, CNRS, Campus Grimaldi, 20250 Corte, France*

^b*INERIS, Parc Technologique ALATA, 60550 Verneuil-en-Halatte, France*

^c*Instituto de Ciências da Terra - ICT (Polo de Évora) & Earth Remote Sensing Laboratory (EaRS Lab), Universidade de Évora, Rua Romão Ramalho, 59, 7000-671 Évora, Portugal.*

ARTICLE INFO

Keywords:


Coupled fire modelling
Fire plume
Multi-scale smoke dispersion
Industrial fire
Air pollution
Atmosphere
Simulation

ABSTRACT

This paper presents an approach to reproduce small to large scale dispersion of smoke induced by industrial fires based on the atmospheric code Meso-NH coupled with the ForeFire surface fire code. Meso-NH can solve explicitly micro to meso-scale meteorology, while ForeFire allows for an efficient parametrization of the injected heat and vapour fluxes. The combination of these two models allows for a straightforward implementation of the heat source term and simultaneously accounts for its effect on local meteorology (as convection and latent heat), thus leading to a prognostic representation of the developing plume. The context of the study imposed to set model parameters that allow for faster than real time forecast along with a qualitatively realistic representation of the plume. Model evaluation in the vicinity of the fire is performed by comparing results with a combustion CFD solver on an idealized situation, followed by a mesh sensitivity study. Then, the proposed coupled method is applied to a real-case multi-scale simulation of smoke dispersion from the local (city) to the continental scale in a twice faster than real-time computation time.

1. Introduction

Many industrial sites, when exposed to uncontrolled fires, are susceptible to provoke immediate and acute impact to the local communities and to heavily contaminate the surrounding environment. An uncontrolled combustion of the stored chemicals may result in the production of heat and pollution creating a rising plume that can affect nearby population immediately through the dispersion of acute toxic products. On longer time scales, spanning from days to years following the accident, the accumulation of pollutants in the environment may result in chronic poisoning. Improving both short and medium term predictions of this type of hazards can help to redefine valuable tools that supports both the short-term emergency response and the post-crisis intervention to assess and circumscribe the environmental damage. Such tools are also possible thanks to recent developments in numerical simulations and increasingly powerful computational resources. However, there are still obstacles to a more systematic use of such numerical simulations when coordinating the short and long-time emergency responses. Firstly, there is an high level of uncertainty characterizing all the different scales involved in the process, especially when considering the short-time scale involved in emergency response. In particular, a relevant forecast of the accident requires a good estimation of chemical emissions (the source term) and of the dynamics of the heat release rate (HRR), including fire suppression activity. Secondly, the time required to compute the desired solutions must be smaller than forecasting time. Satisfying those constraints in an emergency setting imposes that several models and codes are based on many simplifying assumptions. However, this may limit the reliability of the provided predictions, especially when one aims to have an overview on all the involved scales, spanning from the immediate surroundings of the site of the accident, up to the regional scale. A typical example of fast-computing, simplified modelling tools are Gaussian dispersion models, such as the British software ADMS [CHH⁺94] or the American AERMOD [CPV⁺05]. Such models assume a Gaussian distribution of the concentration of pollutants in both downwind and cross-wind directions, given by an analytical solution of the transport equation for an homogeneous, steady flow and a constant point-wise source term, along with hypothesis on the characteristics of turbulent diffusion. This type of modelling provides a fast solution

 baggio_r@univ-corse.fr (R. Baggio); filippi@univ-corse.fr (J.B. Filippi); benjamin.truchot@ineris.fr (B. Truchot); fcouto@uevora.pt (F.T. Couto)

ORCID(s): 0000-0003-1531-0530 (R. Baggio); 0000-0002-6244-0648 (J.B. Filippi); 0000-0003-0175-2100 (F.T. Couto)

describing the diffusion of the pollutants on a medium range spanning from about 10 to 100 km, they can account for terrain topography through suitable parametrizations [Per92], but are known to give poor results when the external wind velocities are low or complex [LMI⁺14]. Lagrangian models are another type of widely used dispersion models accounting for more realistic wind fields which can be taken directly from ongoing meteorological forecasts (see for instance the Micro Swift Spray software [TBO⁺07]). The advective term is determined by the imposed wind field while diffusion is given by a stochastic model of turbulence. With respect to Gaussian models, dispersion models are more expensive but allow to consider realistic meteorological fields and complex terrains. A major drawback characterizing all the above methods is that the convective effect of the heat released by the fire on the local atmosphere is not explicitly resolved. Indeed, industrial fires can release in the atmosphere considerable power (with peaks of several GWs) which modifies locally the wind profile, causing an increase of the vertical lift and of the turbulent flow in correspondence of the fire site. This fire-to-atmosphere interaction is therefore very important for describing properly the height reached by the fire plume and the corresponding diffusion of pollutants. In many cases, the effect of the vertical lift on the rise of the plume is modeled by simple empirical formulas which give an estimate for the height of injection [PWFM16].

As a numerically intense alternative, a detailed description of the combustion process and its influence on the local environment can be evaluated using Computational Fluid Dynamics (CFD) codes that account for combustion. A typical example is the Fire Dynamics Simulator code FDS, developed by the joint efforts of the National Institute of Standards and Technology (NIST) and the VTT Technical Research Centre of Finland [MHM⁺13]. Not surprisingly, the forecast time and spatial dimension are limited to some hundreds of meters maximum, due to the implied computational resources. At the opposite end of the spectrum of involved length scales, spanning from tens of kilometers up to the synoptic scale, numerical weather prediction models (NWP), solving explicitly the equations governing the physics of the atmosphere, can be used to state the diffusion and the interaction of the releasing pollutants with other meteorological and chemical variables. This type of simulations is important in the case of big industrial accidents. For instance, the French code CHIMERE [MMK⁺17] has been used for evaluating the impact of the NL Logistique / Lubrizol industrial fire event in 2019 [RTM⁺21]. However, this type of models is too coarse to represent the effects closer to the accident, in particular they do not solve the convection over a potential fire heat source. At the intermediate (meso-scale) range, several studies used the Weather Research Forecasting model (WRF) [SKD⁺05] coupled with a city sub-grid pollutant dispersion model [NTY21] or with a Lagrangian particle model [KSR⁺22] albeit none explicitly resolving convection at the highest resolution. Wildfire is a specific application for which such micro to meso-scale approach has been already applied successfully from small to large scale events and with models such as WRF/SFire [KMF⁺19] or Meso-NH/ForeFire [FBP⁺11, FBML18]. An example is the simulation performed to predict the evolution of the Aullene Mediterranean wildfire [FBML18], whose computational time did not exceed the time taken by the dynamics of the fire spreading.

In this paper, we propose to develop this latest wildfire approach to model small (near the flame) to large (continental) scale smoke dispersion in case of major industrial fires. At first, a dynamical parametrization of the heat release profile is modeled in the surface fire code ForeFire to account for the typical combustion in such accident. Then, suitable settings, as well as an optimized mesh, are configured for the Meso-NH atmospheric code. For simplicity, we do not inject source terms of chemical species and do not consider the physics of aerosols, despite the fact that suitable models exist in the current versions of Meso-NH [TCS⁺03, TCC⁺05, TGGP06]. We keep track of the evolution of the smoke cloud through the injection of a passive scalar which is emitted at constant rate from the burning domain. Despite its simplicity, such approach allows for a straightforward identification of the effects of the injected heat and vapour on the local meteorological variables, and interactions with the different water phases are observed. The chosen discretization is based on three nested domains, whose resolution varies from 80 m up to 2000 m. This choice allows to model fine meteorological effects near the accident site while simultaneously solving the consequences of the fire on larger scales. To choose the most suitable discretization at the smallest scale, we performed a comparison with a combustion computational fluid dynamics FDS code on an idealized scenario. Then, the modelling tool is applied to the study of a real industrial fire and show that, despite the many length scales involved, it is able to model large scale smoke dispersion.

The paper is structured as follows: The first section presents schematically the two coupled models. Description is limited to the main aspects of both and provide relevant bibliography for more detailed explanations. The second section explores a first simple, small scale application, where we compare mean features of a numerical fire plume simulated respectively with the proposed model and the FDS solver. In the same section, based on this simple setting, results of different Meso-NH grids are compared showing that it is possible to choose a relatively coarse discretization without degrading significantly the representation of the plume in the near field. The third section demonstrates the

feasibility of applying the Forefire/Meso-NH coupled setting to the simulation of a real case with the added advantage of resolving multiple scales simultaneously. The NL Logistique / Lubrizol industrial fire event in 2019 [RTM⁺21] is selected as the study scenario for this purpose. General discussion and perspectives concludes the paper.

2. The coupled fire atmosphere model ForeFire/Meso-NH

The French code Meso-NH (Mesoscale Non Hydrostatic) is a research mesoscale NWP model designed to simulate the relevant physics on a wide range of scales spanning from tens of meters to several hundreds of kilometers [LCM⁺18]. Developed by the joint effort of the Laboratoire de Aerologie and Meteo-France, it is a non-hydrostatic, limited area-model based on the anelastic approximation. The solved equations are the conservation of momentum, mass, water substances and user defined scalar variables, along with a suitably derived thermodynamic equation. The anelastic approximation implies that sound waves are filtered out, thus avoiding the necessity of exceedingly fine time steps in the time integration scheme. The turbulence model used for the parametrization of the unresolved eddies is the scheme proposed by Redespelger and Sommeria [RS81, RS86] (see [CBR00] for details on the implementation). The scheme uses a prognostic equation for the Turbulent Kinetic Energy (TKE), closed by adequate hypothesis on the form of second order turbulent fluxes and the mixing length. The scheme is available both in a simplified 1D version, where the horizontal components of turbulence fluxes are neglected) and in a fully 3D implementation, that is relevant in the smaller scales of this work (lower than $\approx 1 \text{ km}$). Suitable modules allow to study a wide range of physical phenomena, including, among others, the climatic impact of volcanic eruptions, and the electric activity during thunderstorms (see Table 4 of [LCM⁺18] for a detailed overview). At the smaller length scales, the code runs in Large Eddy Simulation (LES) mode to allow an improved representation of turbulence. The meteorological fields imposed at the boundary are taken directly from operational forecast NWP databases (examples of compatible data are the ones obtained by the french model AROME (used in this study) or the European ECMWF). Moreover, the Meso-NH modelling tool allows to account automatically for the local orography and is coupled with the surface model SURFEX. The latter include a physical representation of soil-to-atmosphere heat, water and general exchanges for different surface types (land, town, sea and inland water) [MLMM⁺13].

ForeFire was originally developed to simulate the propagation of wildfires [FBG14]. Its coupling with Meso-NH gives the possibility to inject in the atmosphere arbitrary, time dependent, heat, vapour or any chemical species fluxes, while solving explicitly the convective motions resulting from the interaction with the local atmosphere. The effects of the injected fluxes on the calculated wind fields and on the other meteorological variables are considered explicitly. The flexibility of the ForeFire code allows for a straightforward implementation of ad-hoc routines, suitably designed for the selected release models. Different functions and parameters can be assigned to separate regions of the burning domain, and the dynamics of fire spread can be represented by specifying a suitable *Time of Arrival Matrix* (TAM), which associates a burning starting time at every point in the domain with user defined resolution. Alternatively, one may use very simple maps but specify arbitrary time varying fluxes. Given the flexibility of this time-space tuning, the resulting forcing term can be quite complex and is easily adjusted to assigned dynamic profiles. Once the source terms and the TAM have been specified, the resulting fluxes enter the coupled simulations under the form of time dependent ground forcing terms. We remark that in the case of wildfire spread, a feedback coupling may be necessary, that is, the burning region is adjusted on the basis of atmospheric motions, which, themselves, are driven by the developing fire. This two-way coupling is not relevant for the condition considered here, where the perimeter of the fire hazard is limited by the one of the burning facilities. The most important effects are given by the elevation and the following evolution of the developing plume.

Thanks to the multiscale setting allowed by Meso-NH, we study the diffusion of the plume on multiple length scales simultaneously by using simulations on nested grids. Each grid is characterized by its own with resolution and simulation parameters, in order to model coherently the underlying physics. Before discussing in detail the set-up we used for the multiscale NL Logistique / Lubrizol simulation, we present a simple study concerning the smallest scales of interest. These preliminary tests drove the choice of the parameters used in the finer grids.

3. Coupled simulations results

3.1. Plume evolution in a simple setting

We begin our study on the effectiveness of the ForeFire Meso-NH coupling by studying the development of a fire plume under idealized atmospheric conditions at scales between $\approx 10 \text{ m}$ and $\approx 100 \text{ m}$. In the following subsection, we

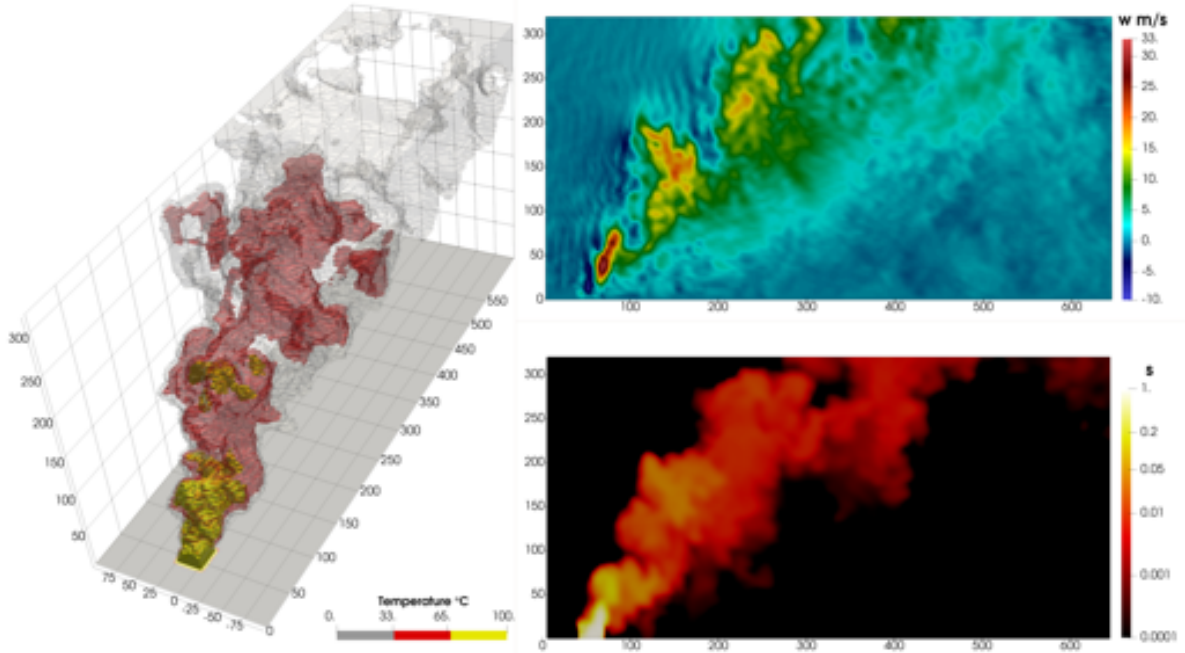


Figure 1: FDS simulation results. On the left: the $s \leq 10^{-3}$ three dimensional subset is presented, colors indicates three different values of temperature. On the right we show the vertical velocity along a X -parallel section along the plane containing w_{max} (on top) the non-dimensional s on an analogous section (bottom), in this latter graph contours are in log scale to improve visualization.

152 draw a qualitative comparison of the plume evolutions calculated by FDS and the one modelled by Meso-NH/ForeFire.
 153 We consider a Meso-NH grid that is much coarser than the one used in the FDS model, despite the fact that Meso-NH
 154 is capable to handle finer grids (see for instance [CRLM21]). This choice is motivated by the fact that we are interested
 155 in providing some confidence in the capability of Meso-NH in solving properly the evolution of the plume with grids
 156 that remain compatible with relatively fast computational times. Indeed, the main purpose of this section is to illustrate
 157 as a relatively coarse Meso-NH grid can model qualitatively well the plume dynamics, once a good estimate of the
 158 HRR has been provided from previous modelling phases. We remark that detailed comparisons between an anelastic
 159 atmospheric model analogous to Meso-NH and FDS has been already discussed in the literature [SJK⁺06]. We limit
 160 our analysis on the main features of the plume, that is, its vertical velocity and the diffusion of the smoke tracer. In
 161 the subsection that follows the representation of the same plume is considered on different Meso-NH grids, which are
 162 made coarser and coarser. The goal is to select a grid that will not filter excessively the main structures inside the
 163 plume. The following examples are based on the simple case of a quadratically increasing heat flux, distributed over
 164 an area of 30 m^2 and reaching a maximum of 3 GW after $t = 150\text{ s}$. The flux then continues steadily. We are interested
 165 in the plume development under a time steady, X -oriented wind profile, representative of a neutral atmosphere and
 166 fixed to a 5D Pasquill class, the velocity then grows from 0 ms^{-1} at ground level up to 5.0 ms^{-1} at the reference height
 167 $Z = 10\text{ m}$, it still grow after based on a power law.

168 3.2. small scale Meso-NH and FDS plume representations

169 To be coherent with the type of modelling adopted by both methods, the evolution of the plume needs to be analyzed
 170 at the scales of the order of some hundreds of meters surrounding the fire. In the coupled model, smoke is described
 171 as a passive scalar which is emitted at constant rate of $1\text{ s}^{-1}\text{ m}^{-2}$ from the heat source where the fire is active, at the
 172 resolution of the given TAM, and is then advected by the convective flow. To make a more relevant comparison with the
 173 "Soot" variable in FDS, we compare these two smoke tracers using their non-dimensional form, obtained by dividing
 174 them by the maximum reached value within the domain.

175 We use a Meso-NH grid characterized by an uniform horizontal discretization $\Delta X = \Delta Y = 40\text{ m}$, and a vertically
 176 varying grid with ground value $\Delta Z_0 = 10\text{ m}$. This grid is progressively enlarged in correspondence of each subsequent
 177 vertical element with constant ratio (here 4%), as typically done in atmospheric models. The simulation is started in

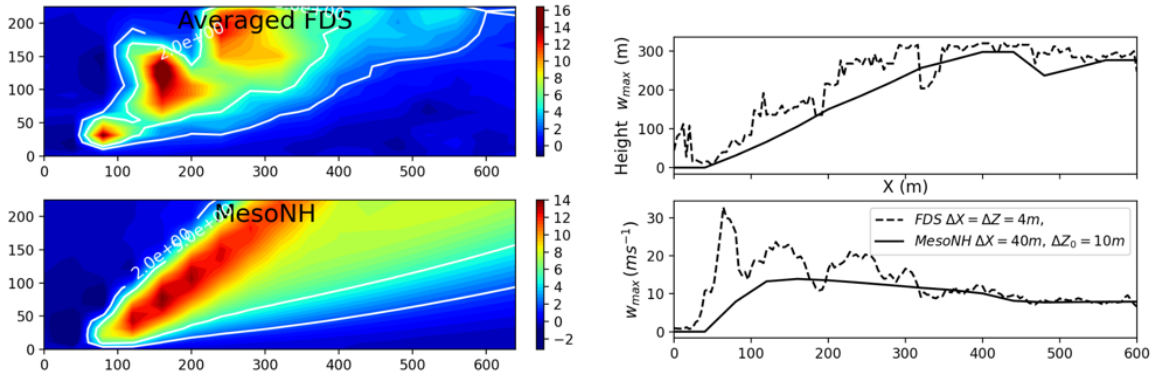


Figure 2: On the left we show w contours for the averaged FDS simulation (top) and Meso-NH (bottom). On the right we show $w_{max}(X)$ and its $Z(X)$ altitude in the two models (FDS results are not averaged).

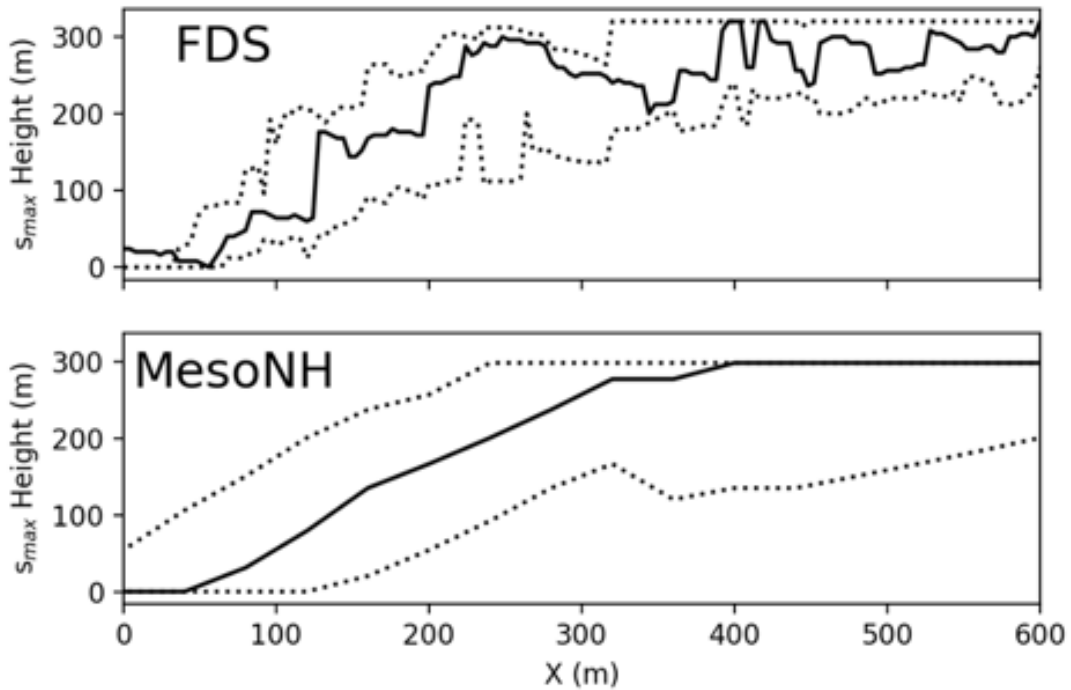


Figure 3: The altitude of s_{max} (continuous line), along with the $s \geq 10^{-3}$ threshold (dotted) for the two models.

178 idealized, stable atmospheric conditions, the assigned wind profile is forced at the boundary with resolution given by the
 179 vertical discretization. The FDS simulation is performed on a much finer grid, with uniform $\Delta X = \Delta Y = \Delta Z = 4\text{ m}$.
 180 The simulated domain is limited to $600\text{ m} \times 600\text{ m}$ horizontally, and to 300 m vertically, to keep low the computational
 181 times. The simulated Meso-NH domain is of about one order of magnitude larger ($8\text{ km} \times 8\text{ km} \times 3\text{ km}$), to lower the
 182 influence of lateral boundary effects. Moreover, such dimensions are comparable to the scales implied in the more
 183 complex models showed later on.

184 The FDS results are schematized on Figure 1, showing the vertical wind velocity w and the distribution of the
 185 scaled soot density s . The vertical sections are taken along planes parallel to X and such that the domain is cut in

186 correspondence of the maximum w and s values respectively. These profiles are taken at time 300 s after ignition, at
 187 which the flame has stabilized. A global view of the plume is illustrated on the left of Figure 1, where only points
 188 such that $s \geq 10^{-3}$ are displayed. One observes clearly the slope imposed by the applied wind field, with the plume
 189 leaving the domain at about 225 m from the emission point. In order to compare the w velocity field with the one
 190 obtained on the coarser Meso-NH plume, the vertical velocity is averaged on a grid analogous to the one used in the
 191 Meso-NH model. Results are shown on the plot in the left of Figure 2. White contours corresponds to the two thresholds
 192 $w = 0.5, 2 \text{ ms}^{-1}$.

193 The coarser grid used on Meso-NH is here clearly incapable to solve the highly turbulent motions, which makes the
 194 velocity field smoother. However, the two cases show a similar maximum value for w , and the two modelled plumes
 195 display comparable slopes. The global agreement between the two simulations is confirmed by the right plot in Figure
 196 2, where the evolution of the maximum value of w with x of the (non-averaged) FDS and Meso-NH are displayed. More
 197 specifically, on the top right graph we illustrate the maximum w value encountered along the X direction, together
 198 with the altitude Z at which such value is encountered (top right graph).

199 In Figure 3, we consider the evolution of non-dimensional smoke tracer s . The continuous line shows the height
 200 at which, in correspondence of each X , the maximum value s is encountered, while the dotted lines are the $s \geq 10^{-3}$
 201 boundaries. On this smoke diagnostic, it is possible to notice a qualitative overall agreement between the two plume
 202 shapes. We conclude that, despite the coarser grid, the Meso-NH model can capture the global properties of the
 203 developing plume, well represented by the trend of the vertical component of the velocity and the associated diffusion
 204 of the smoke term. Both plumes show comparable peak values of w and bend similarly under the action of the imposed
 205 horizontal wind. This aspect is fundamental to explicitly predict smoke dispersion at a larger scale since it governs the
 206 initial height of the fire plume without the need of a parameterized plume-rise model.

207 3.3. Meso-NH plume representation on varying grids

208 In this section, we focus on different Meso-NH representations of the same simple setting discussed before. While
 209 a complete grid sensitivity analysis is beyond the scope of this work, it is still important to estimate how the grid
 210 resolutions affects the plume features, considering the strong impact on the computational time. In particular, the
 211 $\Delta X = \Delta Y = 40 \text{ m}$ discretization previously shown is still relatively costly when one aims to model the plume spreading
 212 beyond the regional scale, even within a suitably designed embedded model. Moreover, the $\Delta Z_0 = 10 \text{ m}$ grid becomes
 213 problematic nearby the heat releasing source, since the ensuing violent convective motions imposes a strong reduction
 214 of the implied time step. We thus consider three different grids with increasing discretization parameters $\Delta X = \Delta Y$,
 215 ΔZ_0 (see labels in Figures 4 and 5), where the finer grid is the same as the one discussed in the subsection above. The
 216 ratio controlling the growing of ΔZ with altitude is 4% in all models. We keep ΔZ_0 relatively low with respect of the
 217 step used in the horizontal direction, to avoid an excessive deterioration in the representation of the plume. All three
 218 simulations consider an horizontal domain of $8 \text{ km} \times 8 \text{ km}$ with elevation $\approx 3 \text{ km}$. In Figure 4 we show the $s \geq 10^{-3} \text{ m}$
 219 representation of the three plumes after the heat flux has become stable ($t > 300 \text{ s}$), while on Figure 5 we illustrate
 220 a vertical cross-section at about 3 km from the fire source, showing the development of a vortex structure. Contours
 221 are proportional to w , (a cutoff between -1 and 1 ms^{-1} has been set to improve the vortex visualization), while the
 222 arrows show the direction of the in-plane component of the wind. We remark that all the three models present the
 223 same qualitative features, with a rising plume which splits with the development of a symmetric structure of rotating
 224 vortexes. While the coarser grid leads to a degraded plume representation, the choice $\Delta X = \Delta Y = 80 \text{ m}$, $\Delta Z_0 = 30 \text{ m}$
 225 is here a reasonable compromise. This is also confirmed by the graphs showed in Figure 6 (analogous to the ones
 226 discussed before when comparing Meso-NH with FDS). On the right, we illustrate the altitude of $w_{max}(X)$ along with
 227 the observed value. On the left we report a schematic representation of the s plumes. The continuous line indicates the
 228 value for which s is maximum, while the dotted lines enclose the $s \leq 10^{-3}$ region.

230 The previous comparison with the FDS simulation shows the ability of Meso-NH to model the initial plume
 231 behaviour in the near field, while the present analysis indicates that decreasing resolution does not strongly modify
 232 its main features. As one could expect, flow and smoke finest structures are filtered out due to the lower resolution but
 233 the upflow mechanism remains well represented and the initial height of the fire plume is in good accordance between
 234 the different cases.

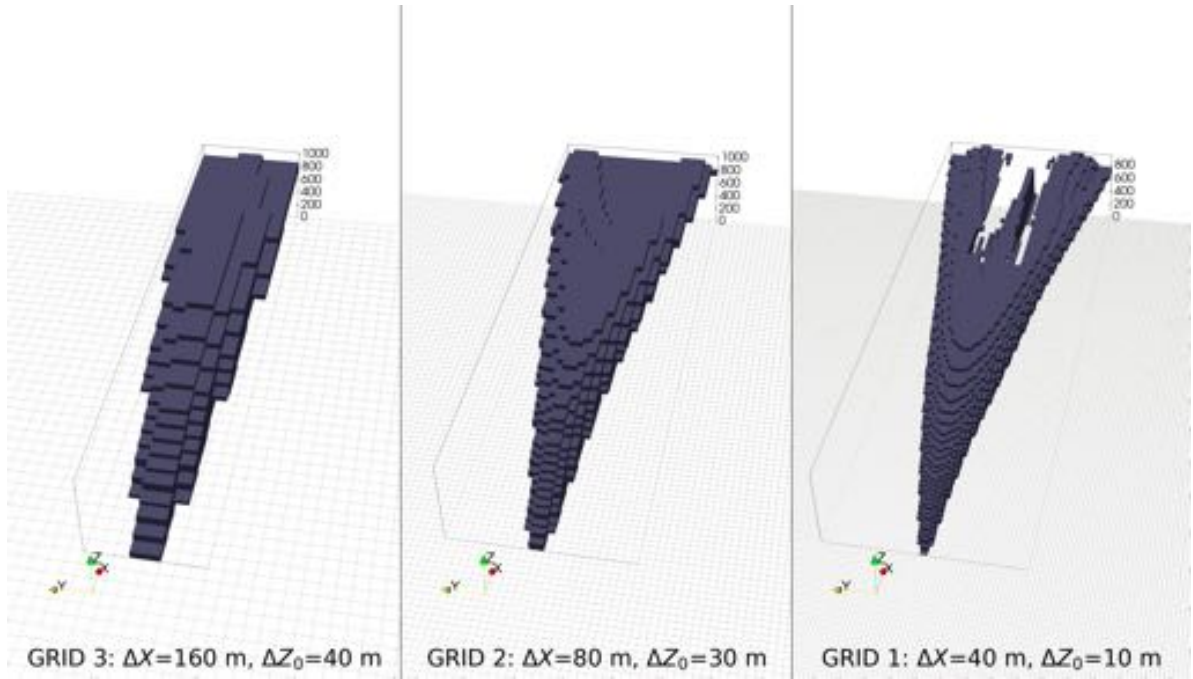


Figure 4: Overview of the three $s \geq 10^{-3}$ plumes (from left to right, coarser to finer grid).

4. Towards real case simulations

In this section, we show the application of the coupled ForeFire/Meso-NH tool to the simulation of the industrial fire which affected the French city of Rouen the 26th September 2019. Due to the chemicals involved in the combustion, firefight actions took almost a day to extinguish it completely, and the fire released in the atmosphere an estimated power of more than 83 *GW h*. The resulting fire plume traveled thousands of kilometers and raised air quality concerns. This choice is motivated by the fact that the Rouen accident is a typical example for which a full-scale atmospheric simulation may give an important support to the organization of the emergency response, and offers a complementary, multiscale tool to the assessment of the resulting environmental damage.

4.1. Main Simulation Settings

In order to resolve properly all the length scales involved in the disaster, we exploit the nesting capability of the Meso-NH software and we subdivide the simulated area in three nested domains with different resolutions (see Figure 7). The horizontal grid size is 2000 *m* for the outer domain covering a total area of 600 *km* × 600 *km*. The inner computational grids have horizontal discretizations of respectively 400 and 80 *m*, over areas of 120 *km* × 120 *km*, and 24 *km* × 24 *km* for the innermost model. The vertical resolution is shared by all the nested domains, with 50 levels up to 20 *km* and a first level above the ground at 30-*m* height. The time step is 10 *s* for the outermost model and decreases to 2 *s* and 0.5 *s* for the finer models. The grid resolution and model parameterisation of the finest domain corresponds to the one used in the idealized configuration analyzed in the previous subsection, and represents here a reasonable compromise between the computational efficiency and the accuracy of the plume representation.

Initial and lateral boundary conditions are provided by the French AROME model (1.3-*km* horizontal resolution) at 0000 UTC, with updates of the coupling files every 3 *h*. The simulation with the coarsest resolution began on 26 September 2019 at 0000 UTC, with a progressive downscaling up to the finest resolution beginning at 0020 UTC.

The burning region determining the site of ignition has been placed in correspondence of the estimated ignition site (see the inset in the right of Figure Figure 7). The total burning area has been set up to 57600 *m*² (corresponding to the bottom of 9 ground elements), which is way more extended than the estimated one (≈ 20000 *m*²). This modelling choice was motivated by the fact that it allows to release the total heat flux while avoiding excessive gradients in proximity of the heat source. This did not affect significantly the physical description, and at the same time allowed to use larger time steps, thus reducing the implied computational time. The assigned burned region is then subdivided in

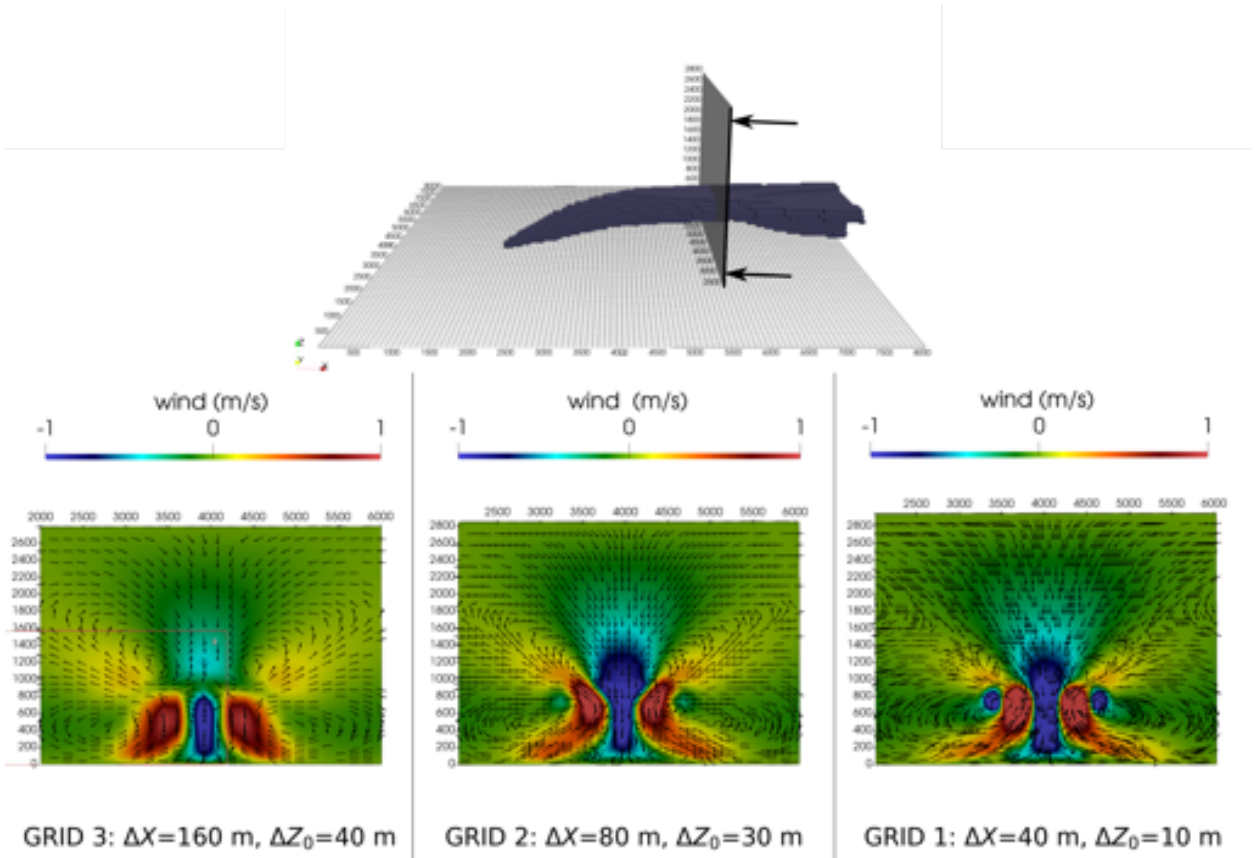


Figure 5: Y-parallel section (illustrated ion top) showing the vortex structure accompanying the plume separation (from left to right, coarser to finer).

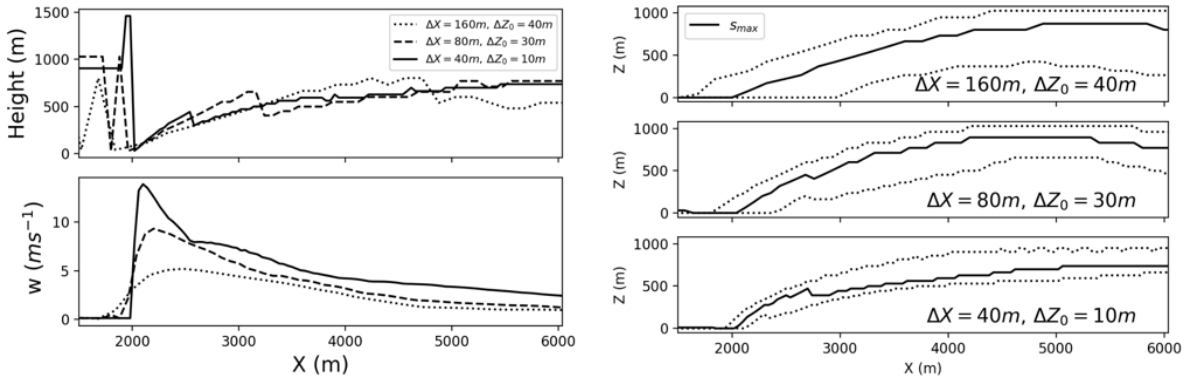


Figure 6: On the left we show the height of $w_{max}(X)$ (top) with the corresponding value (bottom) for the three considered grids. On the right the three $s \geq 10^3$ plume thresholds (dotted) along with the height of s_{max} are showed.

262 two subdomains of different areas, characterized by the same flux model, but with different stating times t_0 (see left
 263 of Figure 8). This simple combination allowed us to obtain the HRR dynamics illustrated on the right of Figure 8,
 264 which is coherent with the estimated dynamics of the fire (including a roof collapse at T+3). The vapour follows an
 265 analogous profile and the total quantity released is coherent with the calculated $\approx 10^4$ t of mineral oil which burned
 266 in the fire (the parameters used in the flux model are: $\phi_{peak} = 250 kW m^{-2}$, $v_{peak} = 0.002 kg s^{-1} m^{-2}$, $t_1 = 1800 s$,

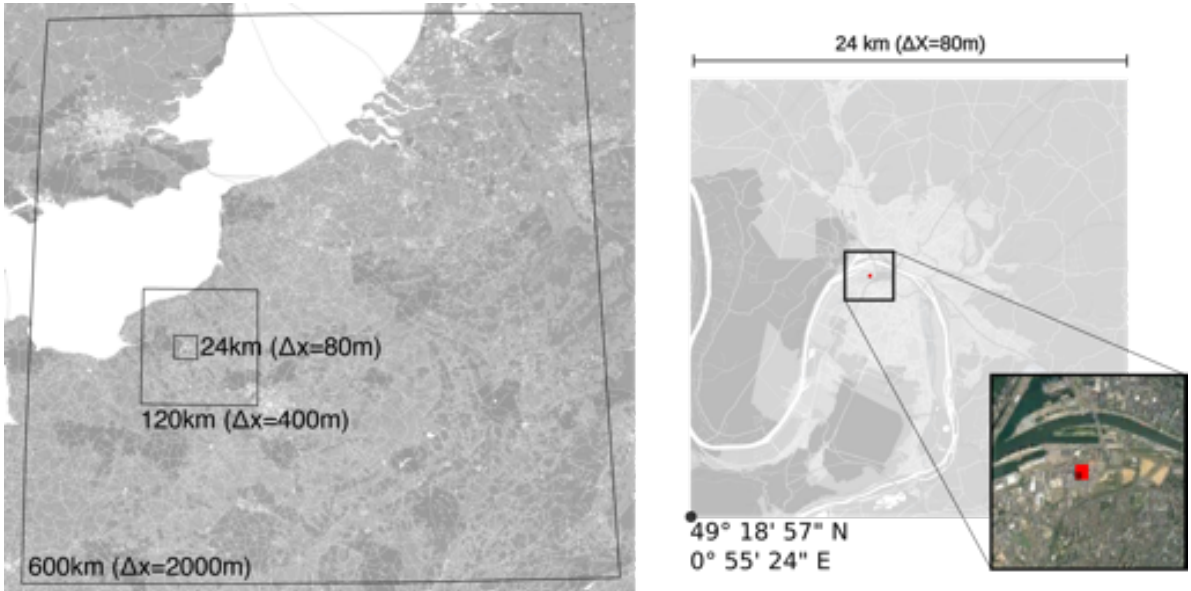


Figure 7: On the left we show the three used nested domains along with the respective discretizations. On the right we show in greater detail the smaller of the nested domain. The inset show the set burning region

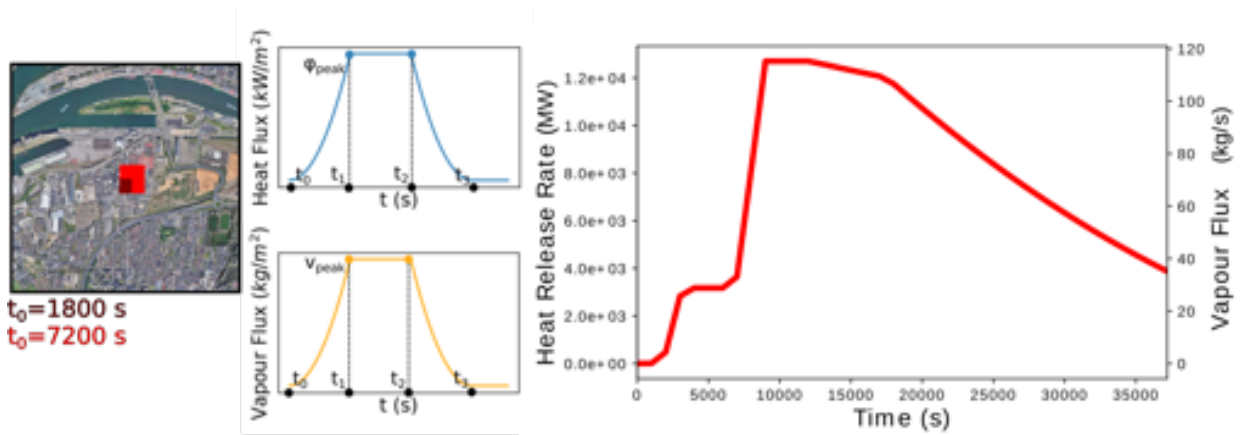


Figure 8: On the left, the implemented burning map along with the time assigned for the arrival of the fire (spread is considered instantaneous within the area). The type of flux function associated with heat and vapor flux is also illustrated. On the right: the corresponding HRR.

267 $t_2 = 18000 \text{ s}$ and $t_3 = 57600 \text{ s}$). We simulated only the first 10 h of the fire, time in which the developing plume reaches
 268 the boundaries of the outermost domain. The total energy released in this laps of time is $\approx 80 \text{ GWh}$.

269 4.2. Dynamical plume structure

270 One of the aims of the current study is to use numerical simulations to better understand fire and atmosphere
 271 interactions and directly solve the updraft caused by the presence of the fire.

272 In Figure 9a) we present two views of the $s \geq 10^{-5}$ and $s \geq 10^{-3}$ plume configurations when the heat release
 273 has reached its peak. As a consequence of the heat injection, the smoke plume is lifted significantly from the ground,
 274 raising up to above 1 km over the site of injection and evolving at similar altitudes. The strength of such lift is important
 275 as the altitude influences the direction of the plume in the zone surrounding the accident. The large scale evolution
 276 of plume is summarized on Figure 9b), which illustrates the $s \geq 10^{-5}$ plume at the end of the simulation, after 10 h
 277 from the ignition. On large distances, the plume rises above 3 km , height that may influence large scale transports of
 278 pollutants. White contours illustrate different s thresholds at the ground level. While the overall plume simulation is

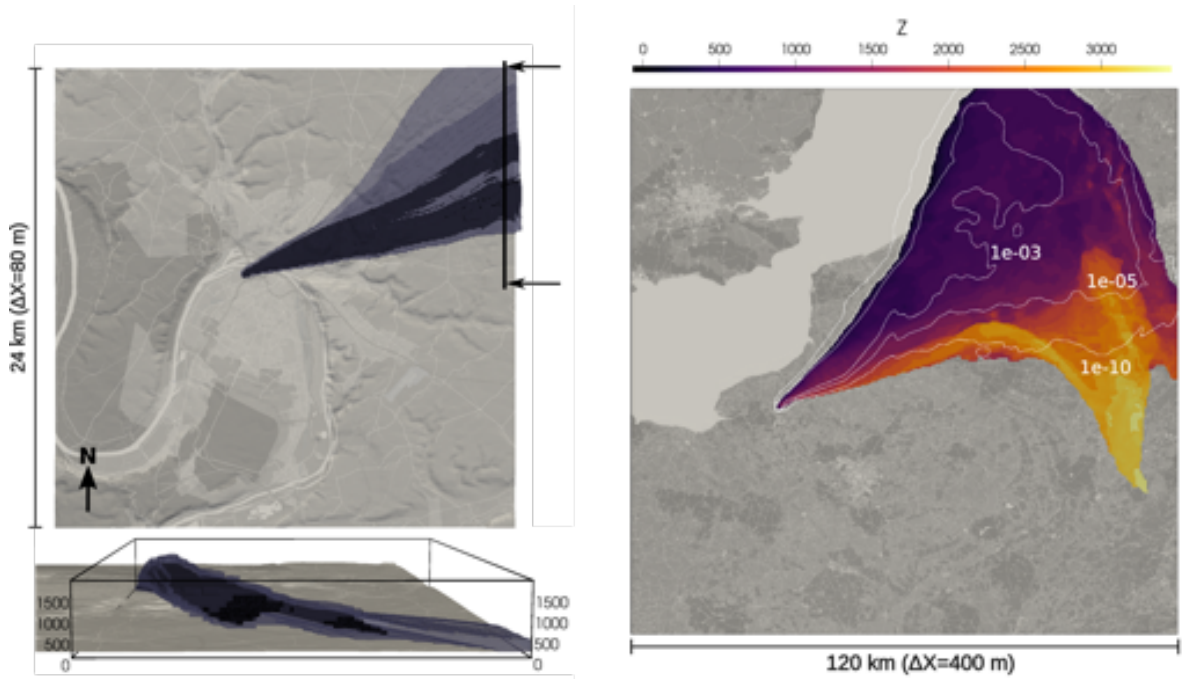


Figure 9: On the left: Plume structure on the smallest of the nested domains. the $s \geq 10^{-5}$ plume is shown using transparent blue while $s \geq 10^{-3}$ is illustrated with solid black. On the right: Evolution of the plume on large scales (colorscale is proportional to the plume altitude). White contours correspond to different s thresholds at the ground.

279 in agreement with previous simulations and observations [RTM⁺21], a complete evaluation of simulation results on
 280 this specific case is beyond the scope of this paper. The main objective of this work is to demonstrate the ability of
 281 the coupled approach to resolve multi-scale plume simulation in a reasonable computational time. An advantage of
 282 Meso-NH with respect of other modelling tools is that it calculates explicitly the interaction between the injected heat
 283 and vapour fluxes and the different water phases present in the atmosphere. We do not consider here the physics and
 284 the chemistry of aerosols, which will be necessary to evaluate more properly the effect of the smoke cloud on the local
 285 precipitation (with a strong impact on computation). However, even in this simpler setting, it is still possible to have an
 286 idea of the regions impacted by fire-related precipitations. In Figure 10 we illustrate the difference between the coupled
 287 simulation and a control simulation (where no heat and vapour fluxes were injected) in terms of total accumulated rain
 288 precipitations at the ground during the 10 hours of the simulated fire, on the intermediate $120\text{ km} \times 120\text{ km}$ nested
 289 domain. It is possible to observe the presence of fire induced precipitations on a region below the one covered by the
 290 plume. It is noteworthy that such a result gives an indication about a possible environmental impact coming from the
 291 deposition of pollutants.

292 4.3. Computational time

293 Computations were performed on the Orsu computer at the University of Corsica (Intel Xeon) composed of 20
 294 nodes of 52 cores each. Faster than real-time (and operational compatible) computation was reached here by running
 295 on 625 processors dispatched in 15 nodes (780 cores mobilized). In this case, it was possible to obtain a 0.5 calculation
 296 ratio with 10 hours of forecast available in 5 hours of computation. This ratio do not take into the generation and
 297 interpolation of boundary conditions that may be already available at the time of alert but would otherwise requires an
 298 additional hour before the simulation can be started (computational time being highly dependent of the resolution of
 299 the data used for these boundary conditions). This 0.5 ratio may limit operational uses, with the first really predictive
 300 output (T+4 forecast) that will technically be available only 3 hours after alert (alert T+3). Nevertheless, as the first
 301 output (forecast T+0) may be available in the first two hours after alert, it may still be useful early, to get an overall
 302 representation of the phenomenon. Moreover, in case of a contained industrial fire, these 3 hours can also be in line
 303 with the time before the breakout of the fire containment (such as a roof collapsing) that is likely to drastically change
 304 plume structure heat release.

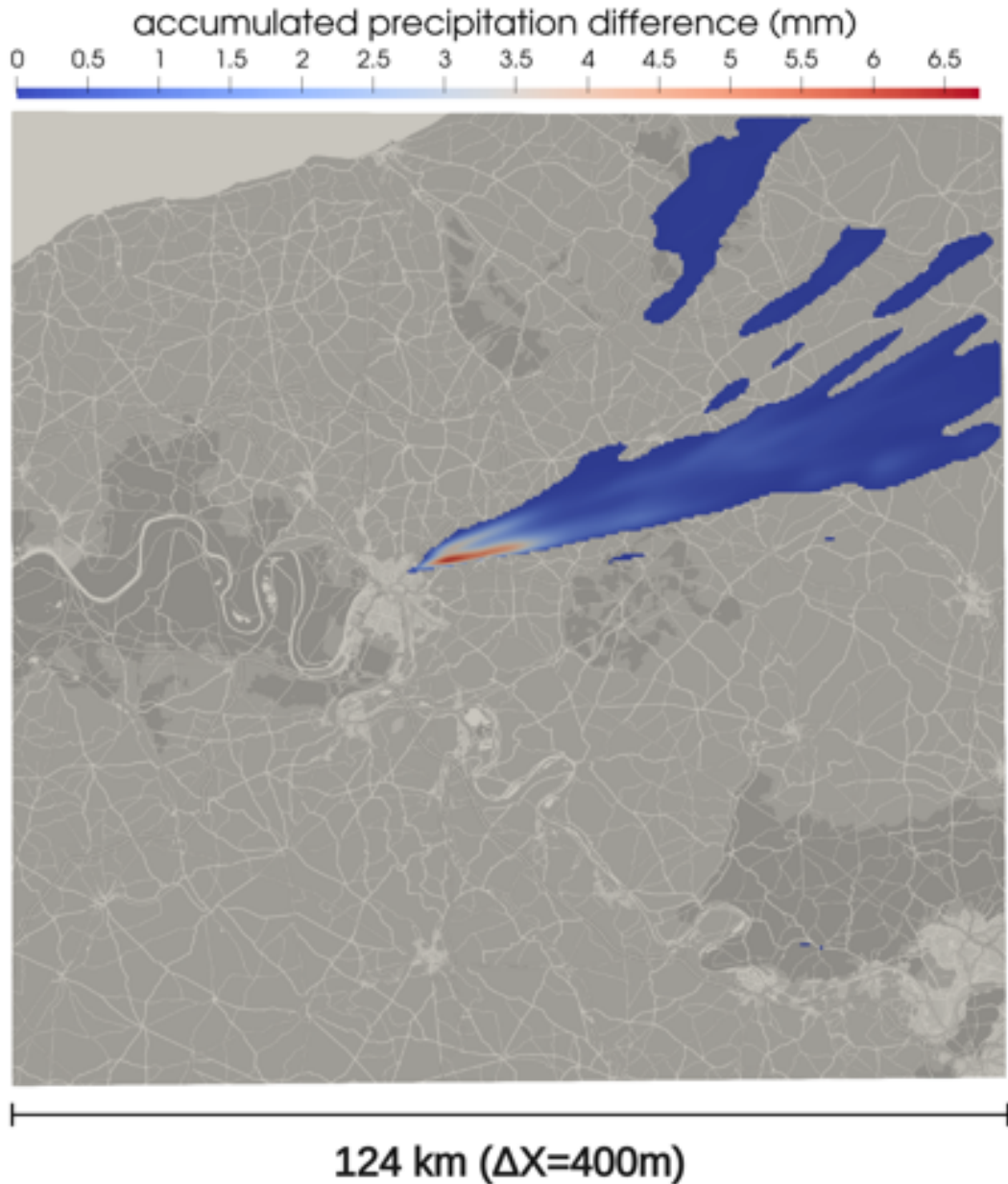


Figure 10: Surplus in total accumulated precipitation (mm) after 10 h of simulation. Landscape features are shown in grey in the background.

305 5. Conclusions and perspectives

306 In this paper we applied the atmospheric code Meso-NH coupled with the ForeFire surface fire code to the
 307 simulation of large industrial fires. The implied Meso-NH model solves micro to meso-scale meteorology, including
 308 convection, turbulence and clouds, in nested domains configurations with resolutions spanning from 80 meters
 309 to 2km. Combustion is resolved here as a sub-mesh fluxes, injected in the atmospheric fields using the ForeFire
 310 model, that computes heat and vapour release at 20 meters resolution using user-defined behavioural functions. Ideal

simulation cases were used to compare to the more detailed, and computationally intensive, FDS combustion code. The comparison shows that the coupled Meso-NH/Forefire simulates coherently the plume convective behaviour near the heat source, at least for heat fluxes of the order of some GWs , which typically characterize industrial fires. The performed real-case simulation illustrates the capability of the proposed MesoNH/ForeFire coupled approach of simulating major industrial accidents, although with some arguable simplifications in the implied physical processes (as for instance the absence of particle injection), and the relatively raw parametrizations of the source terms compared to the complexity of the accident. This multi scale simulation allowed to explore the dynamical structure of the surrounding atmosphere, the strong convection induced by the fire and the related plume lifting, and the interaction with air moisture, creating a rain anomaly under the plume some kilometers away from the source. Although only tested on one real case example, models have been configured, along with grid geometry to be generic for any large industrial fire incident of the same scale. In terms of computational time, the simulation reached a 0.5 ratio (5 hours of computation for a 10 hour forecast) that is therefore predictive, but not instantaneous as simplified tools can provide.

The major point here was to demonstrate the feasibility of such computation with operational forecast constraints, as well as build the platform and configuration to simulate large industrial fires, from local fire release near the source to continental scale smoke transport. Future work is directed to evaluate these specific simulation results by comparing it with in situ observations and existing numerical simulations of the same accident [RTM⁺21]. The proposed approach can be improved by accounting for aerosols and their chemistry, which are known to play an important in precipitation and pollution. On the one hand, the simplified approach used here (a passive scalar) may not be appropriate for precise quantitative estimates of impacts on rain and air quality. On the other hand, the implementation of aerosols physics requires as input an accurate source term with information enough about the characteristics of the combustion products (initial size of the aerosols, gas composition including condensable ones), which may require additional analysis. Finally, the current method could be improved by introducing an automatic procedure to generate the heat release functions or profiles based on the characteristics of the industrial facilities and combustible products involved in the accident.

Acknowledgements: This research is supported by the Agence Nationale de la Recherche, Project ANR-21-SIOM-0010 FirePlume. We thank the super-computing center of the University of Corsica for their support on the computation.

References

- [CBR00] Joan Cuxart, Philippe Bougeault, and J-L Redelsperger. A turbulence scheme allowing for mesoscale and large-eddy simulations. *Quarterly Journal of the Royal Meteorological Society*, 126(562):1–30, 2000.
- [CHH⁺94] DJ Carruthers, RJ Holroyd, JCR Hunt, WS Weng, AG Robins, DD Apsley, DJ Thompson, and FB Smith. Uk-adms: A new approach to modelling dispersion in the earth's atmospheric boundary layer. *Journal of wind engineering and industrial aerodynamics*, 52:139–153, 1994.
- [CPV⁺05] Alan J Cimorelli, Steven G Perry, Akula Venkatram, Jeffrey C Weil, Robert J Paine, Robert B Wilson, Russell F Lee, Warren D Peters, and Roger W Brode. Aermol: A dispersion model for industrial source applications. part i: General model formulation and boundary layer characterization. *Journal of applied meteorology*, 44(5):682–693, 2005.
- [CRLM21] Aurélien Costes, Mélanie C Rochoux, Christine Lac, and Valéry Masson. Subgrid-scale fire front reconstruction for ensemble coupled atmosphere-fire simulations of the fireflux i experiment. *Fire Safety Journal*, 126:103475, 2021.
- [FBG14] Jean-Baptiste Filippi, Frédéric Bosseur, and Damien Grandi. Forefire: open-source code for wildland fire spread models. *Advances in forest fire research*. (Ed. DX Viegas)(Imprensa da Universidade de Coimbra: Coimbra, Portugal), 2014.
- [FBML18] Jean-Baptiste Filippi, Frédéric Bosseur, Céline Mari, and Christine Lac. Simulation of a large wildfire in a coupled fire-atmosphere model. *Atmosphere*, 9(6):218, 2018.
- [FBP⁺11] Jean-Baptiste Filippi, Frédéric Bosseur, Xavier Pialat, Paul-Antoine Santoni, Susanna Strada, and Céline Mari. Simulation of coupled fire/atmosphere interaction with the mesonh-forefire models. *Journal of Combustion*, 2011, 2011.
- [KMF⁺19] Adam K. Kochanski, Derek V. Mallia, Matthew G. Fearon, Jan Mandel, Amir H. Souri, and Tim Brown. Modeling wildfire smoke feedback mechanisms using a coupled fire-atmosphere model with a radiatively active aerosol scheme. *Journal of Geophysical Research: Atmospheres*, 124(16):9099–9116, August 2019.
- [KSR⁺22] Shanu Karmakar, C. V. Srinivas, P. T. Rakesh, R. Venkatesan, and B. Venkatraman. A WRF-FLEXPART simulation study of oil-fire plume dispersion- sensitivity to turbulent diffusion schemes. *Meteorology and Atmospheric Physics*, 134(2), February 2022.
- [LCM⁺18] Christine Lac, Jean-Pierre Chaboureau, Valéry Masson, Jean-Pierre Pinty, Pierre Tulet, Juan Escobar, Maud Leriche, Christelle Barthe, Benjamin Aouizerats, Clotilde Augros, et al. Overview of the meso-nh model version 5.4 and its applications. *Geoscientific Model Development*, 11(5):1929–1969, 2018.
- [LMI⁺14] Adám Leelőssy, Ferenc Molnár, Ferenc Izsák, Ágnes Havasi, István Lagzi, and Róbert Mészáros. Dispersion modeling of air pollutants in the atmosphere: a review. *Open Geosciences*, 6(3):257–278, 2014.

- [MHM⁺13] Kevin McGrattan, Simo Hostikka, Randall McDermott, Jason Floyd, Craig Weinschenk, and Kristopher Overholt. Fire dynamics simulator users guide. *NIST special publication*, 1019(6):1–339, 2013.
- [MLMM⁺13] V Masson, P Le Moigne, E Martin, S Faroux, A Alias, R Alkama, S Belamari, A Barbu, A Boone, F Bouyssel, et al. The surfexv7. 2 land and ocean surface platform for coupled or offline simulation of earth surface variables and fluxes. *Geoscientific Model Development*, 6(4):929–960, 2013.
- [MMK⁺17] Sylvain Mailler, Laurent Menut, Dmitry Khvorostyanov, Myrto Valari, Florian Couvidat, Guillaume Siour, Solène Turquety, Régis Briant, Paolo Tuccella, Bertrand Bessagnet, et al. Chimere-2017: from urban to hemispheric chemistry-transport modeling. *Geoscientific Model Development*, 10(6):2397–2423, 2017.
- [NTY21] Hiromasa Nakayama, Tetsuya Takemi, and Toshiya Yoshida. Large-eddy simulation of plume dispersion in the central district of oklahoma city by coupling with a mesoscale meteorological simulation model and observation. *Atmosphere*, 12(7):889, July 2021.
- [Per92] Steven G Perry. Ctdmplus: A dispersion model for sources near complex topography. part i: Technical formulations. *Journal of Applied Meteorology and Climatology*, 31(7):633–645, 1992.
- [PWFM16] R. Paugam, M. Wooster, S. Freitas, and M. Val Martin. A review of approaches to estimate wildfire plume injection height within large-scale atmospheric chemical transport models. *Atmospheric Chemistry and Physics*, 16(2):907–925, January 2016.
- [RS81] Jean-Luc Redelsperger and Gilles Sommeria. Méthode de représentation de la turbulence d'échelle inférieure à la maille pour un modèle tri-dimensionnel de convection nuageuse. *Boundary-Layer Meteorology*, 21(4):509–530, 1981.
- [RS86] Jean-Luc Redelsperger and Gilles Sommeria. Three-dimensional simulation of a convective storm: Sensitivity studies on subgrid parameterization and spatial resolution. *Journal of the atmospheric sciences*, 43(22):2619–2635, 1986.
- [RTM⁺21] Laurence Rouïl, Frédéric Tognet, Frédéric Meleux, Augustin Colette, Guillaume Leroy, and Benjamin Truchot. Dispersion and impact of smoke plumes from industrial fires: the case of lubrizol. *Environnement, Risques & Santé*, 20(2):126–133, 2021.
- [SJK⁺06] Ruiyu Sun, Mary Ann Jenkins, Steven K Krueger, William Mell, and Joseph J Charney. An evaluation of fire-plume properties simulated with the fire dynamics simulator (fds) and the clark coupled wildfire model. *Canadian Journal of Forest Research*, 36(11):2894–2908, 2006.
- [SKD⁺05] William C Skamarock, Joseph B Klemp, Jimy Dudhia, David O Gill, Dale M Barker, Wei Wang, and Jordan G Powers. A description of the advanced research wrf version 2. Technical report, National Center For Atmospheric Research Boulder Co Mesoscale and Microscale , 2005.
- [TBO⁺07] Gianni Tinarelli, G Brusasca, O Oldrini, Domenico Anfossi, Silvia Trini Castelli, and J Moussafir. Micro-swift-spray (mss): a new modelling system for the simulation of dispersion at microscale. general description and validation. In *Air pollution modeling and its application XVII*, pages 449–458. Springer, 2007.
- [TCC⁺05] Pierre Tulet, Vincent Crassier, Frederic Cousin, Karsten Suhre, and Robert Rosset. Orilam, a three-moment lognormal aerosol scheme for mesoscale atmospheric model: Online coupling into the meso-nh-c model and validation on the escompte campaign. *Journal of Geophysical Research: Atmospheres*, 110(D18), 2005.
- [TCS⁺03] Pierre Tulet, Vincent Crassier, Fabien Solmon, Daniel Guedalia, and Robert Rosset. Description of the mesoscale nonhydrostatic chemistry model and application to a transboundary pollution episode between northern france and southern england. *Journal of Geophysical Research: Atmospheres*, 108(D1):ACH–5, 2003.
- [TGGP06] Pierre Tulet, Alf Grini, Robert J Griffin, and Sebastien Petitcol. Orilam-soa: A computationally efficient model for predicting secondary organic aerosols in three-dimensional atmospheric models. *Journal of Geophysical Research: Atmospheres*, 111(D23), 2006.